

# Supplementary Materials for

## Ecological suicide in microbes

Christoph Ratzke\*<sup>1†</sup>, Jonas Denk\*<sup>2</sup> and Jeff Gore<sup>1†</sup>

<sup>1</sup> **Physics of Living Systems, Department of Physics, Massachusetts Institute of Technology,**

**Cambridge, MA, USA**

<sup>2</sup> **Arnold-Sommerfeld-Center for Theoretical Physics and Center for NanoScience, Ludwig-**

**Maximilians-Universität München, Theresienstraße 37, D-80333 München, Germany**

\*equal contribution

† correspondence should be sent to: [cratzke@mit.edu](mailto:cratzke@mit.edu) or [gore@mit.edu](mailto:gore@mit.edu)

**This PDF file includes:**

Materials and Methods

Supplementary Information

Figs. S1 to S8

## **Material and Methods:**

All chemicals were purchased from Sigma Aldrich, St. Louis, USA , if not stated otherwise.

### Buffer:

For pre-cultures of the bacteria the basic buffer recipe was 10g/L yeast extract (Becton Dickinson, Franklin Lakes, USA) and 10g/L soytone (Becton Dickinson, Franklin Lakes, USA). We refer to that buffer as 1xNutrient medium. The initial pH was 7 and 100mM phosphate were added. For the washing steps and the experiments itself the medium contained 1g/L yeast extract and 1g/L soytone, 0.1mM CaCl<sub>2</sub>, 2mM MgCl<sub>2</sub>, 4mg/L NiSO<sub>4</sub>, 50mg/L MnCl<sub>2</sub> and 1x Trace Element Mix (Teknova, Hollister, USA). We refer to that buffer as base buffer. It was supplemented with phosphate buffer and/or glucose as outlined in the single experiments. The usual concentration was 10g/L glucose, deviations from that are described for the single experiments below. All media were filter sterilized.

### Estimation of Colony Forming Units (CFU):

To estimate the number of living bacteria in the different experiments we used colony counting. At the end of every growth cycle a dilution row of the bacteria was made by diluting them once 1/100x and 6 times 1/10x in phosphate buffered saline (PBS, Corning, New York, USA). With a 96-well pipettor (Viaflo 96, Integra Biosciences, Hudson, USA) 10µL of every well for every dilution step were transferred to an agar plate (Tryptic Soy Broth (Teknova, Hollister, USA), 2.5% Agar (Becton Dickinson, Franklin Lakes, USA) with 150mm diameter. The droplets were allowed to dry in and the

plates were incubated at 30°C for 1-2 days until clear colonies were visible. The different dilution steps ensured that a dilution could be found that allowed for the counting of colonies.

#### pH measurements:

To measure the pH directly in the bacterial growth culture at the end of each growth cycle a pH microelectrode (N6000BNC, SI Analytics, Weilheim, Germany) was used. The grown up bacterial cultures were transferred into 96-well PCR plates (VWR, Radnor, USA) that allowed to measure pH values in less than 200µL.

#### Bacterial culture:

All cultures were incubated at 30°C. The pre-cultures were done in 5mL medium in 50mL culture tubes (Falcon/Becton Dickinson, Franklin Lakes, USA) over night in 1xNutrient described above with additional 100mM Phosphate. The shaking speed was 250rpm on a New Brunswick Innova 2100 shaker (Eppendorf, Hauppauge, USA), the lids of the falcons tubes were only slightly screwed on to allow gas exchange. Except for the 24 h experiment with hourly measurements, which were done in 50mL culture tubes (Falcon/Becton Dickinson, Franklin Lakes, USA), the experiments were all done in 500µl 96-deepwell plates (Deepwell Plate 96/500 µL, Eppendorf, Hauppauge, USA) covered with two sterile AearaSeal adhesive sealing films (Excell Scientific, Victorville, USA), the plates were shaken at 1350rpm on Heidolph platform shakers (Titramax 100, Heidolph North America, Elk Grove Village, USA). The culture volume was 200µL if not stated otherwise. To avoid evaporation the shakers were covered with a custom made polyacryl box (Wetinator 2000) with small water reservoirs placed within.

### Pre-culture and preparation of bacteria:

For these experiments *Paenibacillus sp.* (Ps) was used, a bacterium that can acidify the environment but cannot tolerate low pH values. The bacterium was grown at 30°C. The preculture of Ps was done in 5mL 1xNu, pH 7 with 100mM phosphate for around 14h. Ps was diluted 1/100x into the same medium and grown to an OD/cm of 2. The bacterial solution was washed two times with base with 10mM Phosphate, pH 7. The bacteria were resuspended in the same base and the OD/cm adjusted to 2. The buffer concentration of the base was chosen as detailed in the experiments below.

### 24h experiment with hourly measurement of cell density and pH (Fig. 1):

Tubes were prepared by adding 10ml base with 10g/l glucose and different phosphate concentrations of 10, 14 and 100mM. The bacteria were added by 1/100x dilution. The tubes were incubated at 30°C, 1350rpm shaking. Every hour 200µL were taken from each tube, the CFU was estimated and the pH measured. For every measurement 3 technical replicates were done.

### Density dependence of growth (Fig. 2a):

96-deepwell plates were prepared by adding 200µL base with 10g/l glucose and different Phosphate concentrations ranging from 10 to 100mM (see main text). To obtain different initial densities of bacteria, the bacteria were added by different dilutions ranging from 1/10x to (1/4)<sup>5</sup>/10x dilution. The 96-deepwell plates were incubated at 30°C, 1350rpm shaking. At the beginning of the experiment as

well as after 24h, the CFU was estimated. After 24h the pH was measured. For every condition there are two biological replicates as well as two technical replicates.

#### Growth under daily dilution (Fig. 2B-d):

96-deepwell plates were prepared as for the 'density dependence of growth' experiment. The bacteria were added by 1/100x dilution. The 96-deepwell plates were incubated at 30°C, 1350rpm shaking. At the beginning of the experiment as well as after 24h, the CFU was estimated. After 24h the pH was measured. Every 24h the CFU estimated and the pH were measured and the bacteria were diluted 1/100x into fresh medium. To study the dynamics of bacterial growth and the pH, at the beginning of each day, the bacteria were also diluted 1/100x into a 96-well plate (96 Well Clear Flat Bottom TC-Treated Culture Microplate, 353072, Falcon, Corning, USA) with the same medium in each well as for the 500µl 96-deepwell plate. In addition, every well was supplemented by fluorescent nanobeads (1/100x dilution), which we fabricated as detailed below. In parallel to the incubation of the 500µl 96-deepwell plate, this 96-well plate was then observed in a Tecan infinite 200 Pro (Tecan, Männedorf, Switzerland) at 30°C, 182rpm, 4mm amplitude. Here, the OD was measured via absorbance and the fluorescence of the nanobeads was measured by exciting fluorescein (excitation wavelength 450nm, emission wavelength 516nm) and TFPP (excitation wavelength 582nm, emission wavelength 658nm). Measuring the OD of the bacteria and the fluorescence of the nanobeads every 15min in the course of one day, enabled us to track the change of the pH. Although the OD and fluorescence were measured in the parallel growing 96-well plate, we argue that they (at least qualitatively) capture the dynamics in the 96-deepwell plate, which is underlined by the fact that the measured acidification time and bacterial density oscillate synchronous (Fig. 2d). Parallel to the oscillations in the CFU observed in the 96-deepwell plates, the fluorescence measurements in the 96-well plates display oscillations in the

timepoint, the pH drops, i.e. the timepoints of the fluorescence intensity's turning points (see Fig.2d, Fig. S2).For every buffer condition there were 4 biological replicates in the 96- well and 96-deepwell plates.

#### Fabrication of fluorescent nanobeads:

To study the change of pH during our daily dilution experiments, we fabricated fluorescent nanobeads following a protocol established previously [35]. These nanobeads contain fluorescein, whose fluorescence intensity depends on the pH [36] , and a highly photostable fluorinated porphyrin (TFPP), which acts as a red-emitting reference dye. Since the fluorescence intensity of TFPP is independent of pH it serves as internal standard to make the result independent of the overall nanobead concentration. Thus the ratio of the fluorescein and TFPP fluorescence signals is a function only of the pH value ([35], Fig.S1).

#### Effect of harmful conditions on bacterial survival (Fig. 3):

The pre-culture was done overnight in 1xNutrient, pH7 with 100mM Phosphate. After 15h the bacteria were diluted 1/100x into the same medium. Upon reaching OD/cm 2 the bacteria were washed two times with base buffer and the OD/cm adjusted to 2. The bacteria were diluted 1/100x into 96-deepwell plates (Eppendorf, Hauppauge, USA) containing base medium, pH 7 with 10g/L glucose and different amounts of Kanamycin, NaCl or Ethanol. For Fig. 3a the glucose concentration was varied. The bacteria were incubated for 24h at 30°C, 1350rpm on a Heidolph platform shakers (Titramax 100, Heidolph North America, Elkove Village, USA) as described above. The live cell density was estimated

via colony counting upon start of the experiment and after 24h. The pH was measured after 24h with a pH microelectrode as described above.

#### Frequency of ecological suicide (Fig. 4):

For this experiment 22 different soil bacteria were used, which were identified out of 119 soil bacteria (Logan ref) to yield the highest change in pH. To make this selection, the precultures of the 119 soil bacteria were done in 200 $\mu$ L 1xNu, pH 7 with 100mM phosphate for 14h at room temperature, 800rpm shaking. The precultures were then diluted 1/100x into the same medium and grown for 6 hours, which approximately corresponded to a growth to an OD/cm of 2 for the precultures of Ps used in the Ps experiments detailed above. The bacteria were then diluted 1/100x into fresh medium and grown for 24 hours at room temperature, 800rpm shaking. After 24 hours, the bacterial density (CFU/ml) and pH of all cultures were measured and the 22 bacteria with the highest change in pH were selected.

For these 22 species, precultures were done in 5mL 1xNu, pH 7 with 100mM phosphate for 14h. The cultures were diluted 1/100x into the same medium and grown to an OD/cm of approximately 2. The bacteria were resuspended in the same base and the OD/cm adjusted to 2. To categorize the species according to 'suicidal', 'self-inhibiting', 'self-supporting' and 'neutral' each species was grown in the same base once with high buffer concentration (100mM phosphate) and once with low buffer concentration (10mM phosphate). At the beginning and after 24 hours, the CFU was estimated. The pH was measured after 24h with a pH microelectrode as described above.

## Supplementary Text

In these Supplementary Notes we further elaborate our dynamical analysis of ecological suicide in microbes. We first discuss the dependence of the fluorescence intensity of our fabricated nanobeads (see Methods) on the pH. Then, we present time resolved measurements of the optical density and the fluorescence intensity of these nanobeads throughout our daily dilution experiments.

To test our conceptual understanding of ecological suicide in *Paenibacillus sp.* (Ps), we present a mathematical description based on our experimental observations. We show that the proposed mathematical equations capture the complete phenomenology of ecological suicide in Ps, including non-monotonic growth dynamics and oscillatory behavior in daily dilutions.

### *Paenibacillus sp.* isolation and phylogeny:

The *Paenibacillus sp.* was isolated from a grain of soil collected in Cambridge, MA, USA and was part of a soil species collection that will be described in more detail elsewhere (Logan Higgins et al, in prep). The 16S rRNA of this strain was sequenced and is most closely related to *Paenibacillus tundrae* A10b [37] according to RDB/SeqMatch tool [38] with a similarity score of 0.995 and a S<sub>ab</sub> score of 0.975.

### Dependence of the nanobeads' fluorescence intensity on the pH:

To study the dynamics of the pH, we fabricated fluorescent nanobeads (see methods) which show a pH-dependent fluorescence intensity [35]. These nanobeads contain fluorescein, whose fluorescence intensity depends on the pH, and a highly photostable fluorinated porphyrin (TFPP), which acts as a



red-emitting pH independent reference dye. Since the fluorescence intensity of TFPP is independent of pH it serves as internal standard to make the result independent of the overall nanobead concentration. Thus, the ratio of the fluorescein and TFPP fluorescence signals is a function only of the pH value. Since in our 24-hours experiments the pH varied between 4 and 7, we measured the fluorescence intensity ratio of the nanobeads for different pH values in this range. The fluorescence intensity ratio increases monotonically for increasing pH. Moreover, the slope of the intensity ratio decreases for decreasing pH and the intensity seems to saturate for low pH (Fig. S1).

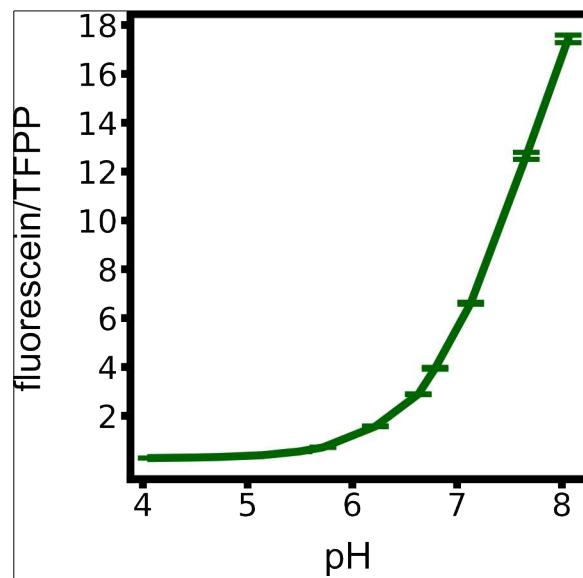


**Fig. S1:** *The nanobeads' fluorescence ratio of fluorescein and TFPP depends on the pH. Rescaling the fluorescein signal with the TFPP signal shows a monotonic increase as a function of the pH. The fluorescence of the nanobeads was measured in base medium with adjusted pH values as shown on the x-axis. Errorbars show the SEM of 8 independent replicates.*

Dynamic measurements of the optical density and pH:

As detailed in the main text (Fig. 2c-e), our daily dilution experiments show oscillatory behavior of the bacterial density, which was measured at the end of each day. In contrast, we could not observe significant oscillations in the pH at the end of each day, i.e. for a certain buffer concentration, the pH after one day was approximately constant (Fig. S2).

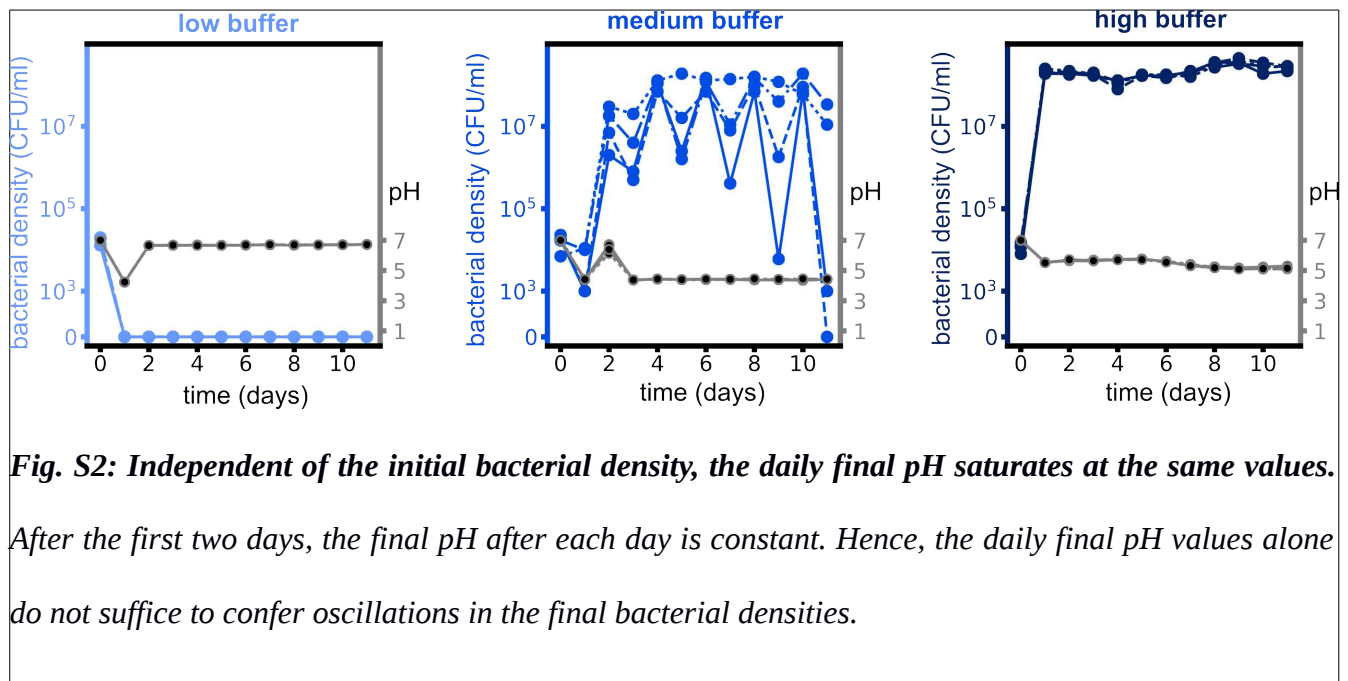


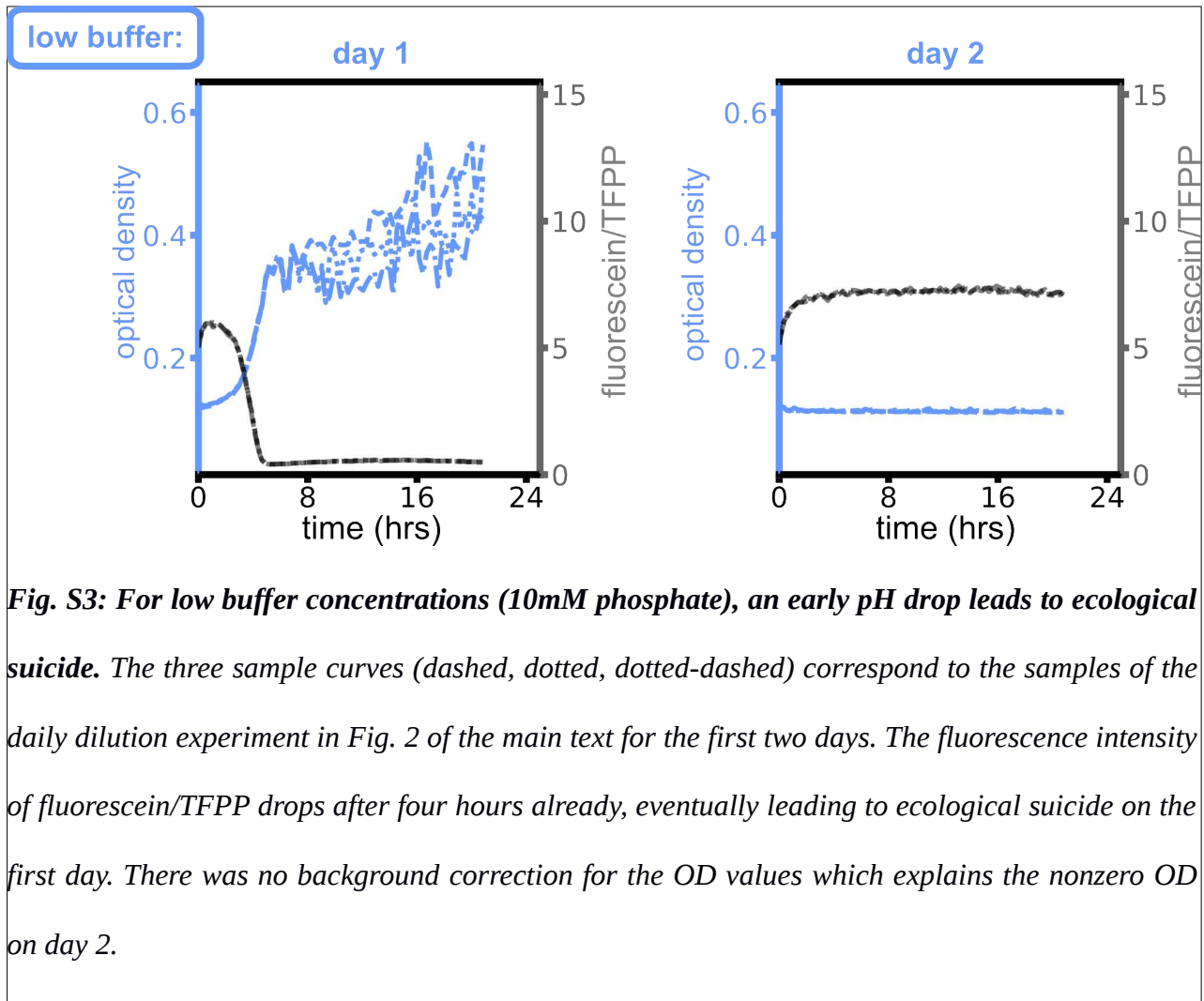
**Fig. S2: Independent of the initial bacterial density, the daily final pH saturates at the same values. After the first two days, the final pH after each day is constant. Hence, the daily final pH values alone do not suffice to confer oscillations in the final bacterial densities.**

This suggests that from the pH values at the end of each day it is not possible to infer the (oscillating) behavior of the bacterial density. Therefore, we also studied the dynamics of the pH during the course of each day during our daily dilution experiment. To this end, we prepared parallel experiments with the same buffer conditions and initial bacterial dilutions as for the daily dilution experiments (see Methods). In contrast to the daily dilution experiments, to these parallel experiments we also added fluorescent nanobeads and measured the optical density and fluorescence intensity of the nanobeads (see Methods). Whereas for the bacterial density (CFU/ml) at the end of each day we counted the living bacteria, the optical density provides a measurement for the total amount of bacteria (dead and alive).

As detailed above (Fig. S1), the fluorescence intensity ratio of the nanobeads provides a measure for the pH.

For very low buffer concentrations (10mM phosphate), our daily dilution experiments (Fig. 2 left) display ecological suicide during the first day already. Consistently, in the corresponding parallel experiment with fluorescent nanobeads we find an early and strong decrease of the fluorescence intensity ratio after four hours of the first day already (Fig. S3), indicating a strong decrease in pH (Fig. S1). This drop in pH is accompanied by a rapid increase of the optical density. On the second day (and all following days), the optical density mostly stays constant for the entire day. This strongly suggests that the bacteria have died on the first day already, which is underlined by finding no viable cells via plating on rich medium agar (Fig. 2c). In all measurements of the nanobeads' intensity ratio, we find an initial rapid increase. We argue that this initial increase is due to the initial increase in temperature during the initial heating of the PlateReader to 30°C. When suspended in pure base (without bacteria)

we indeed observed an increase of the fluorescence signal of the nanobeads for increasing temperature (Fig. S4).





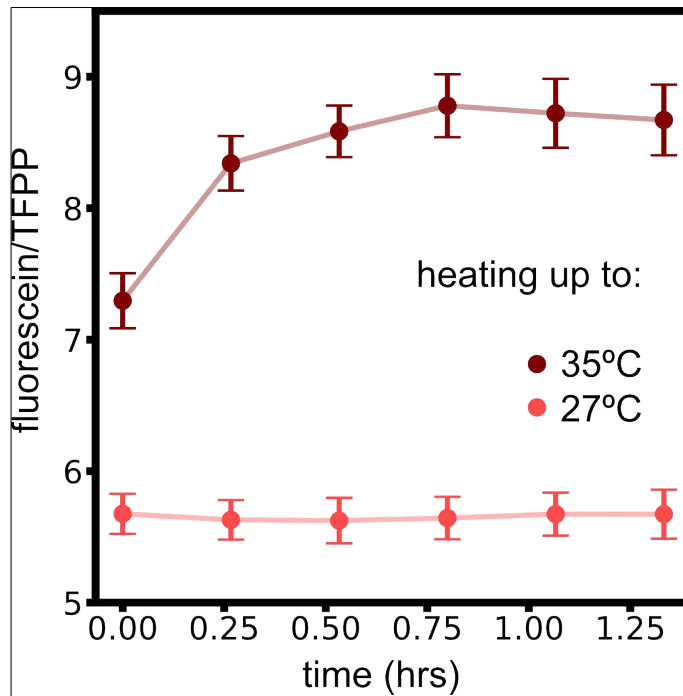


**Fig. S4:** The fluorescence intensity ratio of the nanobeads is temperature dependent. The temperature dependence rationalizes the initial increase of the fluorescence intensity ratio in Fig. S3 and Fig. S5. The fluorescence of the nanobeads was measured over time in base buffer at pH 7. First the nanobeads were incubated at 27°C until a stable value could be obtained. Afterwards the temperature was increased to 35°C and the measurement continued. The increase in temperature is followed by a increase in the fluorescence ratio, which shows that the signal is temperature dependent. Mean and SEM of 10 replicates are shown.

For high buffer concentrations, the optical density and the nanobeads' fluorescence intensity show a similar respective increase or decrease on each day (Fig. S5 a,c). This is consistent with the daily saturation of the bacterial density observed in our daily dilution experiments (Fig. 2e). As mentioned above, for intermediate buffer concentrations we could observe oscillations in the bacterial density but not in the pH at the end of each day (Fig. S2). However, our parallel experiments with fluorescent nanobeads reveal oscillatory behavior of the time the fluorescence intensity--and thus also the pH--drops (acidification time, which is defined as the turning point of the resulting S-shaped fluorescence ratio curve). A late drop of the fluorescence is accompanied with a high final bacterial density in the



daily dilution experiment and an early drop with a low final bacterial density. Hence, for intermediate buffer concentration the acidification time in our parallel experiment oscillates with the bacterial density in the daily dilution experiment (Fig. S5).

Mathematical approach to ecological suicide:

As detailed in the main text, our conceptual understanding of ecological suicide is based on the following principles: bacterial growth leads to a change in their environment (pH) in a way that eventually harms themselves and leads to their own death. Hence, bacteria experience a negative

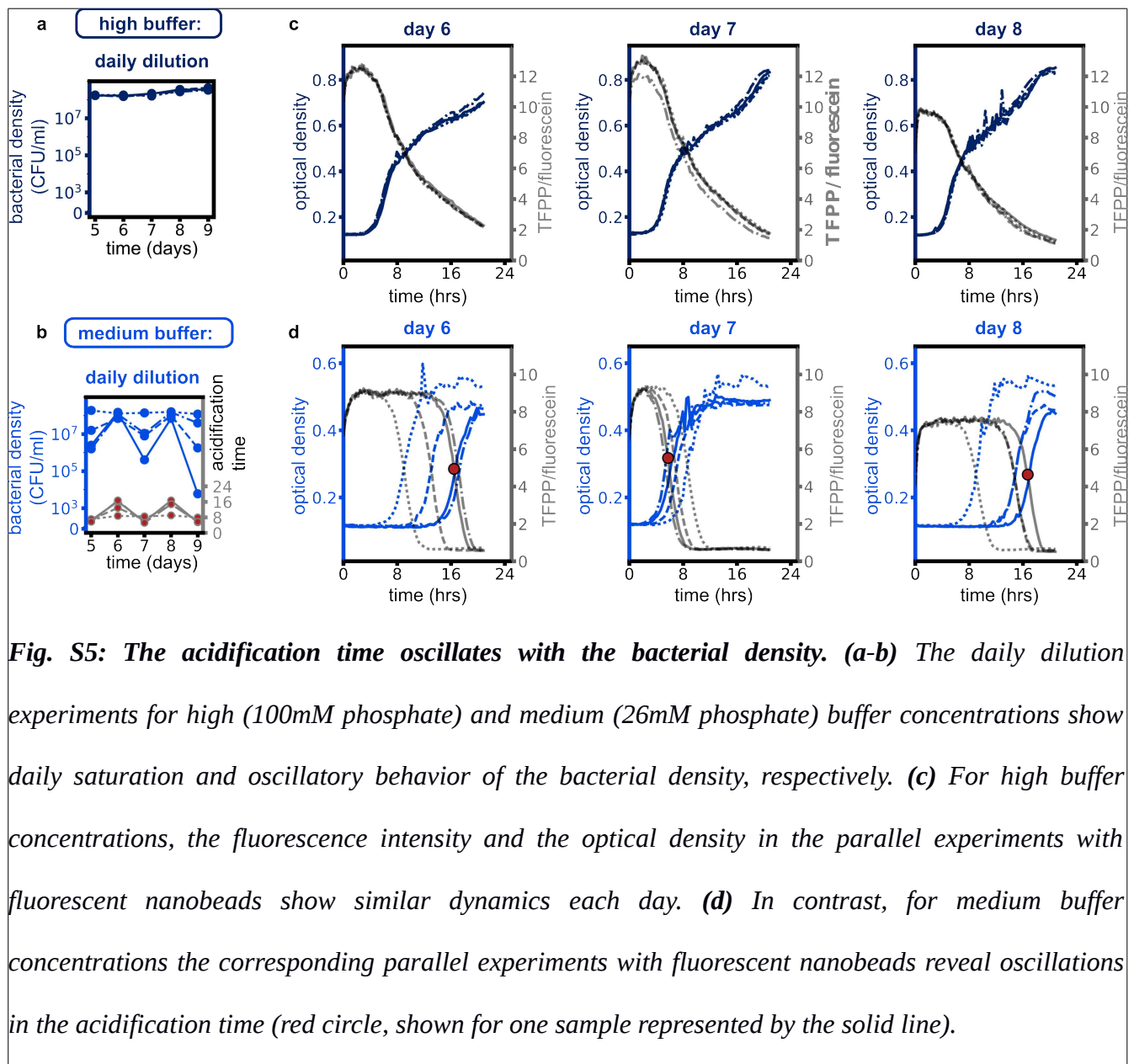


**Fig. S5: The acidification time oscillates with the bacterial density.** (a-b) The daily dilution experiments for high (100mM phosphate) and medium (26mM phosphate) buffer concentrations show daily saturation and oscillatory behavior of the bacterial density, respectively. (c) For high buffer concentrations, the fluorescence intensity and the optical density in the parallel experiments with fluorescent nanobeads show similar dynamics each day. (d) In contrast, for medium buffer concentrations the corresponding parallel experiments with fluorescent nanobeads reveal oscillations in the acidification time (red circle, shown for one sample represented by the solid line).

feedback mediated by the surrounding pH. It is important to note that we do not seek a complete description of ecological suicide including all the molecular details, but rather want to test our conceptual understanding (negative feedback) on a phenomenological level. Here, we show that from a mathematical perspective, ecological suicide is a very generic phenomenon, which can be captured by a minimal extension of previous mathematical descriptions of bacterial growth [5]. Bacteria have an optimal pH value where they grow best [8,9]. Deviations from this value deteriorate their growth and can even cause their extinction. To account for this pH dependence of bacterial growth, we propose the following dynamics for the bacterial density  $n$ :

$$\frac{dn}{dt} = \alpha n \left(1 - \frac{n}{\kappa}\right) \Gamma[p] \quad , \quad (1)$$

where  $\alpha$  and  $\kappa$  are the growth rate and the carrying capacity, respectively, and the function  $\Gamma[p]$  depends on the proton concentration  $p$  and represents the effect of the proton concentration (pH) on the bacterial growth. For a fixed  $\Gamma[p]$ , this equation is the well-studied logistic growth with growth rate  $\alpha\Gamma[p]$  and carrying capacity  $\kappa$ . One ad hoc choice to account for a pH dependence of the bacterial growth is to assume that the deterioration of bacterial growth with changing proton concentration follows a Gaussian. Here, we define

$$\Gamma[p] := 1 - \frac{\left(1 - \exp\left[\frac{(p - p_{opt})^2}{2\sigma^2}\right]\right)}{\left(1 - \exp\left[\frac{(p^c)^2}{2\sigma^2}\right]\right)} \quad , \quad (2)$$

where  $p_{opt}$  denotes the optimal proton concentration and  $p^c$  denotes some critical proton concentration deviation beyond which bacteria start to die. All of these proton concentrations are not in physical units but instead is simply meant to capture the dynamics of the proton concentration.  $\sigma$  determines how far from the optimal proton concentration the species can grow / survive. Based on the strong correlation between the increase in the optical density and the fluorescence intensity ratio (Fig.

S3 and S5), we assume that the change in pH—and thus the proton concentration—is directly related to the growth of the bacteria. A naive assumption would therefore be that the change in proton concentration is simply proportional to the change in bacterial density and is completely determined by eq. (1). However, note that in this case the system reduces to a system of only one dynamic variable (the bacterial density  $n$ ) which would not be able to reproduce non-monotonic growth [39] as observed in our experiments (Fig. 1). There are many ways to implement a negative feedback of the proton concentration on the bacterial density capable of reproducing non-monotonic behavior as observed in our experiments [39, 40]. The goal of our mathematical description is not to account for the molecular details of the process, which would involve the complex (and largely unexplored) metabolism of the particular bacteria under consideration (in our case *Paenibacillus sp.*). In contrast, our goal is to develop a simple mathematical model that delivers intuition about the dynamics of ecological suicide in *Paenibacillus sp.* and test its consequences especially in the light of the experimental findings like non-monotonous growth and oscillations.

Fig. 1c displays a decrease of the pH even after saturation of the bacterial density and thereby suggests, that the proton concentration also couples to the bacterial density itself. Since, in principle,

the proton concentration could depend on both the change of the bacterial density  $\left(\frac{dn}{dt}\right)$  and the bacterial density  $(n)$  itself, we make the following approach for the dynamics of  $p$  :

$$\frac{dn}{dt} = \beta_1 \left(\frac{dn}{dt}\right) \Theta \left[\frac{dn}{dt}\right] + \beta_2 n, \quad (3)$$

where  $\beta_1$  and  $\beta_2$  are (real, positive) coupling parameters.  $\Theta[\cdot]$  denotes the Heaviside step function, which is one for a positive argument and zero otherwise and accounts for our assumption that bacteria increase the proton concentration during their growth, but do not affect the pH when they die. Whereas high  $\beta_1$  and  $\beta_2$  will yield a fast increase in the proton concentration with bacterial

growth and total density respectively, for very low  $\beta_1$  and  $\beta_2$  the proton concentration will hardly change. We therefore assume a decrease of  $\beta_1$  and  $\beta_2$  to emulate an increase in buffer concentration in our experiments. This model is thus an extension of the simpler model used in [10]. Measuring time, bacterial density and proton concentration in units of  $1/\alpha$ ,  $\kappa$ , and  $p_{opt}$ , respectively, the only independent parameters are the rescaled coefficients coupling  $p$  to  $\frac{dn}{dt}$  and  $n$  given by  $\beta'_1 = \beta_1 \kappa / p_{opt}$  and  $\beta'_2 = \beta_2 \kappa / (\alpha p_{opt})$ , respectively, the rescaled critical proton concentration deviation  $p^c / p_{opt}$ , and the rescaled spread  $\sigma^2 / p_{opt}^2$ . Fig. S6 a-c show the dynamics of the bacterial density and the proton concentration as a function of time for a certain time interval  $24/\alpha$ , which is proposed to simulate daily growth. In all simulations we chose the same values for  $p^c / p_{opt} = 0.6$  and  $\sigma^2 / p_{opt}^2 = 1$ , assumed the initial proton concentration to be optimal and only varied the coupling coefficients  $\beta'_1$  and  $\beta'_2$ . For convenience, the proton concentration is plotted as  $-\log(p)$ , which is up to some scaling the corresponding pH of the system. Similar to our experimental observations for increasing the buffer concentration (compare to Fig.1 a-c), decreasing the coupling of the proton concentration to the bacterial density (by lowering  $\beta'_1$  and  $\beta'_2$ ) shows a transition from a rapid decline of the bacterial density for strong coupling to saturation of the bacterial density at the carrying capacity for weak coupling (Fig. S6a-c). Note, that due to the continuous description, the bacterial density  $n$  cannot reach 0 (extinction) but only approaches 0 at infinite times. However, from our daily dilution experiments (Fig. 1c) we can estimate the carrying capacity with approximately  $10^8$  cells; hence bacterial densities below  $1/10^8 \kappa$  would correspond to less than one cell. We therefore claim that bacterial densities below  $1/10^8 \kappa$  correspond to extinction in our experiments and manually set the bacterial density to zero, if it is lower than  $1/10^8 \kappa$ . Starting at different initial conditions, the fold growth of the bacteria is decreasing for increasing initial

concentrations (Fig. S6d), as observed in our experiments (Fig. 2a). Similarly, there is a critical maximal initial density above which the bacteria start to die out (the fold growth drops below 1). Similar to our experiments, this reciprocal dependence of the initial to the final density leads to interesting behavior when simulated in a "daily dilution" simulation: Here, we numerically integrated equations (1) to (3) for  $24/\alpha$ , which in line with our above simulations represents one day of our experiments. To account for the 1/100x daily dilution, the final bacterial concentration is multiplied by a factor of 1/100 and then taken as the initial bacterial density of the subsequent simulation. Note, that this procedure can be understood as a discrete map for the bacterial density, where - apart from the dilution factor of 1/100 - the mapping is given by the relation of the bacterial density at  $t = 24/\alpha$  and  $t = 0$  as given in Fig. S6d. Discrete maps show a rich phenomenology ranging from stable fixed points and limit cycles to chaos and can be very sensitive to the form of the mapping function [41]. Similarly, we expect that changing the form of the mapping function (Fig. S6d) by changing the coupling constants  $\beta'_1$  and  $\beta'_2$  is critical for the long-term behavior in our daily dilution simulations. In view of the similar shapes of this mapping (Fig. S6d) and the well-studied logistic map [42] we speculate that for a very shallow shape--as it occurs for weak coupling (small  $\beta'_1$  and  $\beta'_2$ )--the discrete map approaches a stable fixed point, whereas for a steep (negative) slope due to strong coupling (large  $\beta'_1$  and  $\beta'_2$ ) the bacterial density will diverge until it eventually takes values below  $1/10^8 \kappa$  (extinction). For intermediate slopes, i.e. for intermediate values for  $\beta'_1$  and  $\beta'_2$ , the daily dilution simulations may show oscillations between multiple values. Fig. S7 shows respective bifurcation diagrams of our daily dilution simulations when varying the coupling constants  $\beta'_1$  and  $\beta'_2$  continuously. These bifurcation diagrams display bifurcations from one stable fixed point to oscillations between two values of the bacterial density. Also our experiments suggest bifurcations between a fixed final bacterial density and oscillations between multiple values (Fig. S8). Due to the sensitivity of logistic maps against a change in the mapping function and due to natural

noise in our experiments, we note however that a quantitative categorization of the oscillations observed in our experiments (Fig. 2d) in terms of limit cycles of the underlying discrete map (Fig. 2a) may not be feasible and is beyond the scope of this work.

In our daily dilution simulations, for very strong coupling of the proton concentration to the bacterial

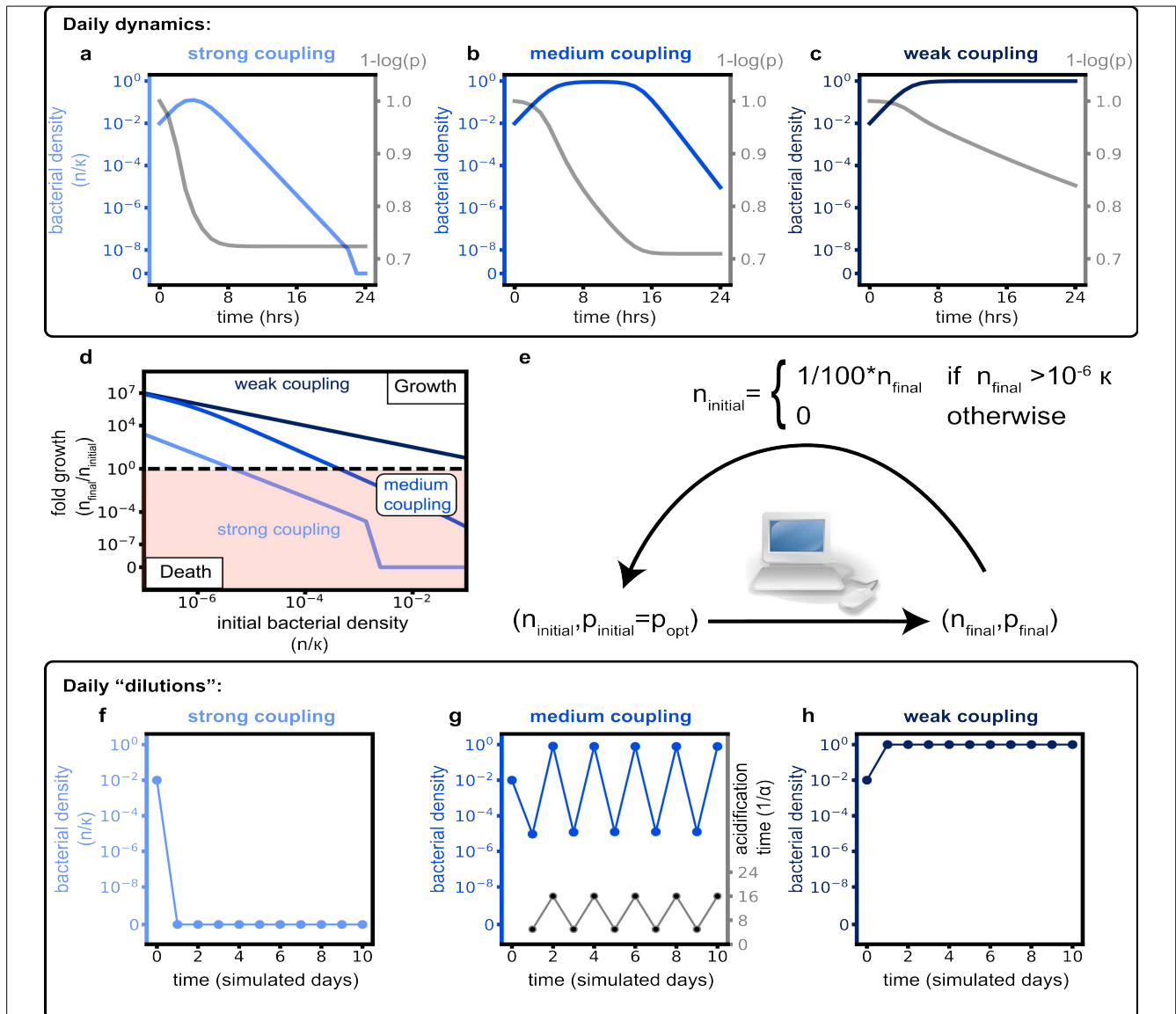


**Fig. S6: Negative feedback of the pH on the bacterial density suffices to recapitulate the phenomenology of ecological suicide as observed experimentally.** **a-c**, Based on eq. (1)-(3), strong (  $\beta'_1=3, \beta'_2=1$  ), medium (  $\beta'_1=0.24, \beta'_2=0.08$  ), and weak (  $\beta'_1=0.06, \beta'_2=0.02$  ) coupling has a similar effect on the growth dynamics as low, medium and high buffer concentrations in our experiments (Fig. 2c-e). **d**, The fold bacterial growth decreases for increasing initial concentration. When simulated in a "daily dilution" scheme. If the cell number that is 'diluted' at the end of the day dropped below one cell – this is possible since the variables are continuous in differential equations – the bacterial density was set to zero. **e**, this reciprocal dependence leads to similar scenarios, **f-h**, as observed experimentally (Fig. 2, c-e).

density (  $\beta'_1=3, \beta'_2=1$  ), the bacterial density dramatically decreases on the first "simulation day" already (Fig. S6f). Due to our continuous description, the bacterial density does not reach zero. However, note that the bacterial density drops below  $1/10^8 \kappa$ , which corresponds to extinction as detailed above (to account for this extinction, we therefore manually set the density to zero). For medium coupling (  $\beta'_1=0.3, \beta'_2=0.1$  ), We find oscillations in the final bacterial density (Fig. S6g), reminiscent to our daily dilution experiments with intermediate buffer concentration (Fig. 2d). Furthermore, we find, that the acidification time (the time of the turning point in the proton concentration) oscillates with the bacterial density. For weak coupling (  $\beta'_1=0.06, \beta'_2=0.02$  ), the bacterial density saturates at the carrying capacity after the first day already and all subsequent "simulation days" (Fig. S6h), as observed in our experiments with high buffer concentration (Fig. 2e). The phenomenological agreement between our mathematical description and our experiments strongly suggests, that the coupling of the bacterial density and the environment (here the pH) and the resulting non-monotonic growth dynamics are key aspects in understanding the phenomenon of ecological suicide.



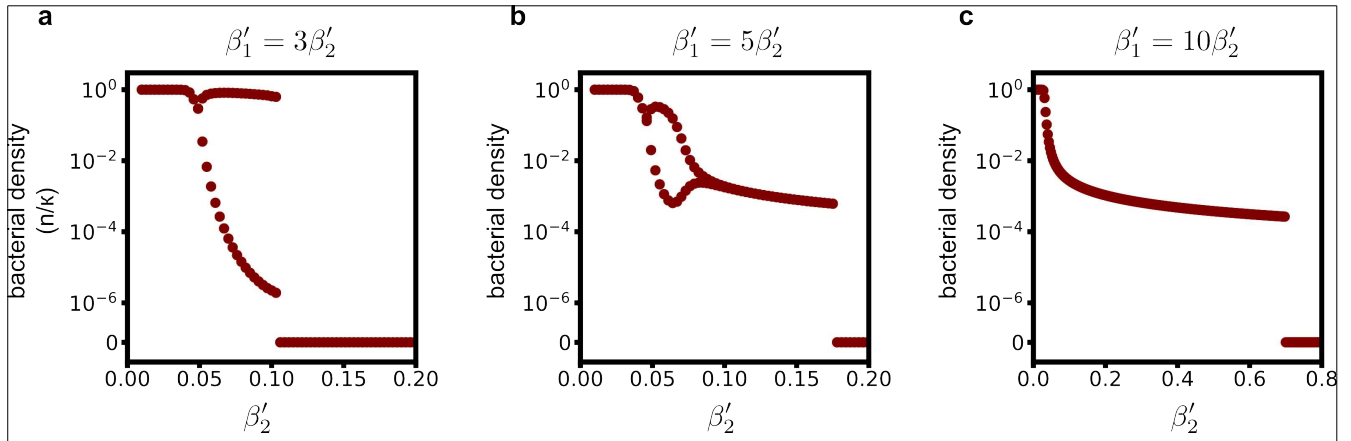


**Fig. S7: Varying the coupling constants  $\beta'_1$  and  $\beta'_2$  shows bifurcations from one fixed point to oscillations between two points.** The bifurcation diagrams show the values of the bacterial density at the end of the last two days after 'daily dilution' simulations corresponding to 60 days. **a**, For comparable coupling constants (here:  $\beta'_1=3\beta'_2$  , as used in Fig. S6), the discrete mapping of 'daily dilution' simulations displays a bifurcation from one stable fixed point (saturation) to oscillations between two points. When a 1/100 dilution would cross the cutoff of  $1/10^8\kappa$  (i.e. if after any of the 60 simulation days  $n < 1/10^6\kappa$  ), the bacterial density was manually set to zero. **b**, For an intermediate ratio  $\beta'_1/\beta'_2=5$  , the amplitude of oscillations first increases and then decreases again for increasing  $\beta'_2$  . **c**, For high enough  $\beta'_1/\beta'_2$  (here:  $\beta'_1/\beta'_2=5$  ) the coupling to the change of bacterial density is dominant and the system saturates at low final densities, but shows no oscillations (recall that strong enough coupling to the bacterial density itself is crucial in our equations (3) to generate oscillations). In b, and c, the bacterial density drops below the extinction cutoff after the first first day already when  $\beta'_2$  is too high.

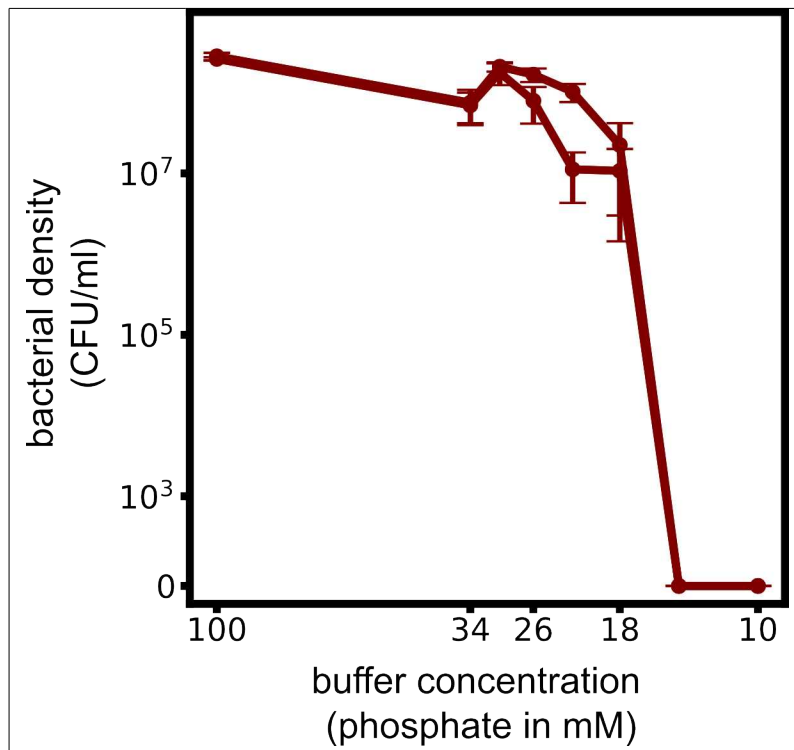


**Fig. S8: Experiments suggest a bifurcation between stable bacterial density at the end of each day and oscillations.**

The 'bifurcation diagram' shows the mean amplitude of the final bacterial density on the last day (day 11) and the second last day (day 10) for different buffer concentrations. The mean and SEM of the 4 replicates also used in Fig. 2 are shown.